

Dynamics of emerging functional shifts in cooperative systems

Author: Cristina Sastre Jachimska

Facultat de Física, Universitat de Barcelona, Diagonal 645, 08028 Barcelona, Spain.

Advisor: Dr. Josep Sardanyés (Centre de Recerca Matemàtica), Dr. M. Carmen de Miguel

Abstract: Hypercycles are cyclic catalytic systems formed by replicating species, conceived in the 1970's as a solution to the so-called information crisis or Eigen's paradox. So far, hypercycles have considered only cooperation, together with the emergence of so-called catalytic short-circuits and parasites. More recently, the impact of functional shifts (the change from cooperation to degradation or predation by one of the species) has been investigated in both discrete- and continuous-time systems. These previous models, however, included these shifts in an implicit manner, assuming that some species or a given fraction of them changed cooperation. Here a simple model for a two-species hypercycle is proposed, in which one of the species explicitly produces a degrader phenotype due to mutational processes, where the effects of cleavage and predation have been studied. We have identified a saddle-node bifurcation separating coexistence from co-extinctions, involving bistable dynamics before the bifurcation occurs. Although the effects of predation have been found to be damaging, cleavage turns out to be, to some extent, beneficial.

I. INTRODUCTION

Dynamical systems and mathematical models are key to understanding how the biological, biophysical and chemical world works. The hypercycle is a mathematical and biological model first proposed as a possible solution to the error threshold paradox for the RNA-based abiogenesis hypothesis, by the biophysical chemist Manfred Eigen in the 1970's [1] [2]. In this hypothesis, RNA macromolecular replicators (ribozyme-like molecules) are thought to be the first carriers of genetic information. Nevertheless, there was found to be a limit in the length of self-replicators, set by the catastrophic genetic information loss due to high mutation rates. However, current organisms dispose of enzymatic mechanisms for correcting errors introduced by random mutations, allowing them to preserve genetic information above such a limit (the error threshold). Those mechanisms, at the same time, can only be developed by genetically complex organisms. This is called the *Eigen paradox*.

The basic hypercycle model has been widely studied and fundamentally consists of cyclically organised self-replicating macromolecules, as opposed to non catalytically-coupled quasispecies. In hypercycles, each replicator catalyses the replication of the next one. Due to cooperation (by catalysis) among the different ribozymes, the stability of the whole ensemble is enhanced. This results in a higher resistance to the loss of information by mutation, thus in being capable of storing a higher information content beyond the error threshold. Therefore, the model proposes the evolution and persistence of the whole system, rather than that of single molecules, as a solution to this paradox. The formation of complex ribozyme networks has also been observed experimentally over the past decades [3] [4].

The system studied in this project is proposed as an extension to the predatory model in [5]. It consists of a two-species catalytic cycle without autonomous self-

replication, where one of the species generates a mutant which shifts its interaction strategy from cooperation to cleavage/predation. New to this work is the mutation being considered explicitly over time, generating a third species. The system also presents a certain death rate and logistic growth regulation due to limited landscape carrying capacity. The system will be studied from both continuous-deterministic (mean field model) and discrete-stochastic (CA model) points of view in order to study the effects of mutation and predation/cleavage in well-mixed and spatially-resolved systems.

Aside from its original object of study, the hypercycle model has also been used in other fields as ecology, economy or sociology. From an ecological point of view, the dynamics proposed in this project can be commonly found in natural ecosystems. Behavioural changes as described above can happen due to environmental or climatological circumstances in order to ensure the species' survival. For example, some seabirds which present intraspecific cooperation to find nourishment, also exhibit predation during breeding in colonies, the intensity of which depends on climatological conditions [6].

II. MODELS

A. MATHEMATICAL MODEL

The hypercycle studied in this work consists of three cyclically-organised, catalytically-interacting species, S_1 , S_2 , S_3 , without autonomous self-replication. That is, all replication processes are hetero-catalytic. Species S_3 , which is generated over time due to mutation from S_2 , has acquired a functional change allowing it to cleave or predate on species S_1 . Hence, species S_1 catalyses the replication of S_2 and S_3 and, at the same time, is catalysed by S_2 and cleaved/predated by S_3 . Thus, the system contains both cooperative and cleaving/predating

dynamics. The general model is given by:

$$\begin{cases} \frac{dS_1}{dt} = k_{12}S_1S_2\theta(\vec{S}) - \epsilon S_1 - k_{13}S_1S_3, \\ \frac{dS_2}{dt} = (1 - \mu)k_{21}S_2S_1\theta(\vec{S}) - \epsilon S_2, \\ \frac{dS_3}{dt} = (\mu k_{21}S_2S_1 + \alpha k_{13}S_3S_1)\theta(\vec{S}) - \epsilon S_3. \end{cases} \quad (1)$$

Where all constants are positive and defined as follows:

- k_{ij} : catalytic reproduction/degradation rate by S_j on S_i .
- ϵ : death rate of the species. It has been considered equal for all species for the sake of mathematical simplicity, and taken as $\epsilon = 0.05$.
- μ : mutation rate from S_2 to S_3 , with $\mu \in [0, 1]$.
- α : predation benefit by S_3 on S_1 . As the amount of benefit can never exceed the amount of exerted degradation, $\alpha \in [0, 1]$. $\alpha \neq 0$ corresponds to $S_3 \rightarrow S_1$ predation, whereas $\alpha = 0$ corresponds to cleavage. Cleavage and predation differ in the absence and presence of benefit from degradation.
- $\theta(\vec{S}) = 1 - \sum_i S_i/C_0$: logistic growth regulation term, with carrying capacity $C_0 = 1$.

The parameters of main interest for our analyses are μ , k_{13} and α , corresponding to the effects of explicit mutation, cleavage and predation. When $\mu = 0$, no mutant is generated and the system is reduced to a 2-species hypercycle without autonomous self-replication [5]. On the other hand, when $\mu = 1$, the totality of species S_2 mutates to S_3 and the system becomes entirely cleaving/predating. As neither of the species has autonomous self-replication, the system will go to extinction.

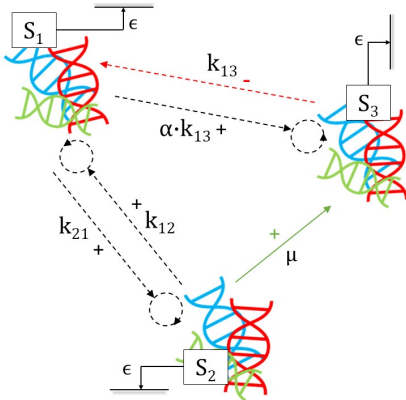
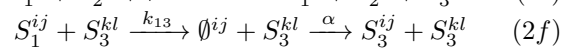
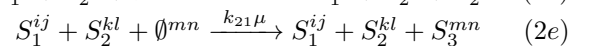
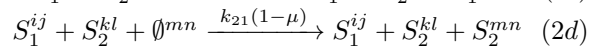
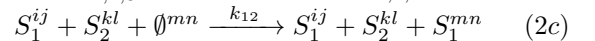
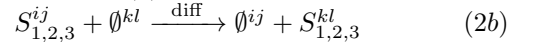


FIG. 1: Interactions considered in our models: black arrows represent cross-catalytic interactions, red arrows represent directed degradation or predation, green arrows represent mutation, and solid thin black arrows spontaneous degradation. The constant rates/probabilities for each process are shown

B. CELLULAR AUTOMATON

The cellular automaton represents a time-discrete, spatially-explicit, stochastic approach to the model presented above. Let Ω be an $N \times N$ dimensional lattice, the state space, where each cell of the lattice can take the values $\Omega_{i,j=1,\dots,N} \in \{\emptyset, S_1, S_2, S_3\}^{i,j}$.

Let \mathcal{N}_{ij} be the neighborhood of the cell (i, j) and let the four nearest cells $k, l, m, n \in \mathcal{N}_{ij}$. Periodic boundary conditions have been assumed. The evolution of the system is such that at each iteration a random cell is selected from the lattice. Depending on the state found at the cell $\Omega_{i,j}$, the following set of reactions can take place:



Where the reactions hold for spontaneous degradation (2a), diffusion (2b), $1 \leftrightarrow 2$ catalysis (2c, 2d), $2 \rightarrow 3$ mutation (2e), $1 \leftrightarrow 3$ cleavage/predation (2f), with its respective probability coefficients, with *diff* being the diffusion rate.

III. RESULTS

A. Mathematical model

1. Equilibrium points and stability: analytical results

Despite the complexity of the interactions the mathematical model presents, and knowing the results from [5], some general considerations can be extracted from an analytical treatment.

From studying the nullclines intersection (where $\dot{S}_{i=1,2,3} = 0$) one can find the equilibrium points of the system. It is easy to see that $\vec{S}_0 = (0, 0, 0)$ is an equilibrium point.

Linearising the system and evaluating the Jacobian matrix, \mathbb{J} , at \vec{S}_0 , its eigenvalues λ have been computed by $\det(\mathbb{J} - \lambda\mathbb{I}) = 0$ where \mathbb{I} is the identity matrix. It has been found $\lambda = \{-\epsilon, -\epsilon, -\epsilon\}$. Considering the Jacobi stability criterion, the equilibrium point $\vec{S}_0 = (0, 0, 0)$ has all its eigenvalues negative and, therefore is always locally asymptotically stable. Thus, in the parameter range where another stable solution exists, the system will present bistability, where the evolution outcome will highly depend on the initial conditions.

Also, there is no possible non-negative solution with only 1- or 2-species extinction, i.e. the system only presents either total coexistence or total co-extinction.

This can be easily seen as, imposing any $S_i = 0$ leads either to the extinction of the other species, or to inconsistencies like $S_j < 0$, as all species populations are defined as positive and the equilibrium points must lay inside the first quadrant.

The general solution $\vec{S} = \vec{\Phi}(x) \mid \vec{S} \neq (0, 0, 0)$ is not presented due to high parametrical complexity and length, but the following conclusions can be drawn. There are three potentially positive solutions that can be described in terms of $x = x(k_{ij}, \alpha, \mu, \epsilon)$. It is interesting to notice that two of the x solutions are complex conjugates, yet they remain real in the range of study.

2. Numerical results

In this section, a numerical approach to studying the dynamics and stability of the model will be presented, where the cleaving and depredate systems will be compared. RK4-5 integration methods for time evolution and *numpy python* numerical linearisation algorithms have been used. Stability surfaces in $\mu - k_{13} - S_i$ space and bifurcation diagrams (Figure 2 and Figure 3), as well as time and phase-space trajectories (Figure 4 and Figure 5) have been computed. Considering the analytical results, the $\vec{S} = 0$ surface is always stable for $\forall \epsilon > 0$. Furthermore, after carrying out an exhaustive numerical computation, it has been observed at most two simultaneous real, stable fixed points, i.e. bistability.

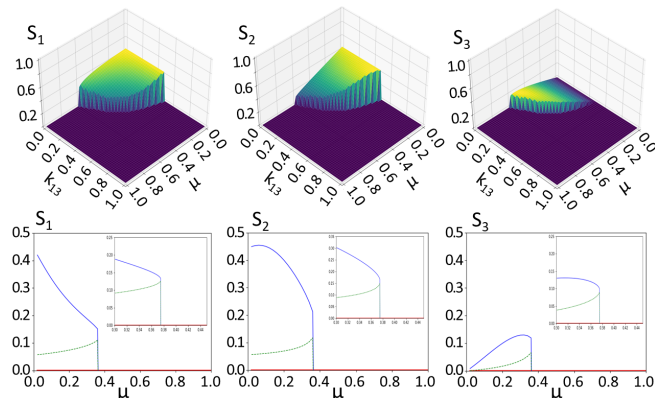


FIG. 2: Dynamics of Eqs. (1) for the case with cleavage, taking $\alpha = 0$ and with S_1 , S_2 and S_3 from left to right. *Top row:* $\mu - k_{13}$ phase portrait for $k_{21} = 1.0$; $k_{12} = 1.0$, showing the stability surface for initial conditions $\vec{S}_0 = (0.5, 0.5, 0.5)$. *Bottom row:* Sliced bifurcation diagram μ , with $k_{21} = 1.0$; $k_{12} = 1.0$; $k_{13} = 0.5$, with the respective closeups in the critical point's neighborhood. The continuous lines represent stable fixed points and the green dashed line, an unstable fixed point.

For the case with cleavage (Figure 2) the mutation parameter, μ , mainly reduces the S_1 and S_2 equilibrium populations due to the increase of the mutation, until an S_3 threshold is reached before phase transitioning. There is a small range for which S_2 population increases,

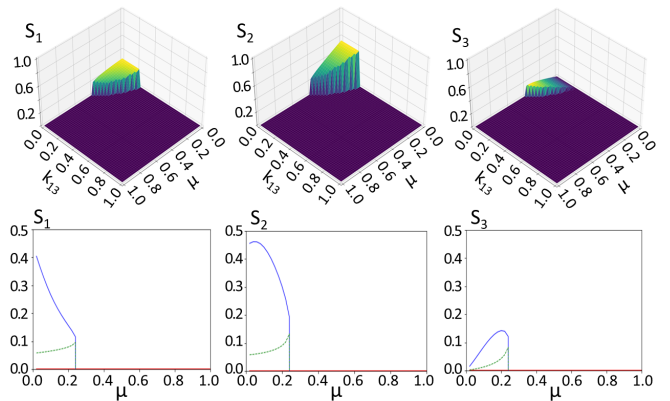


FIG. 3: Dynamics of Eqs. (1) for the case with predation, with $\alpha = 0.75$ and with S_1 , S_2 and S_3 from left to right. *Top row:* $\mu - k_{13}$ phase portrait for $k_{21} = 1.0$; $k_{12} = 1.0$, showing the stability surface for initial conditions $\vec{S}_0 = (0.5, 0.5, 0.5)$. *Bottom row:* Sliced bifurcation diagram for μ , with $k_{21} = 1.0$; $k_{12} = 1.0$; $k_{13} = 0.5$. The continuous lines represent stable fixed points and the green dashed line, an unstable fixed point.

therefore mutation can result beneficial for the system in small measure. The increase of the cleavage parameter, k_{13} , reduces the value of the critical point. The effect of adding the non-symmetry $k_{12} \neq k_{21}$ is the reduction of the bistability area under the surface. Thus, the system loses stability due to catalysis unbalance between S_1 and S_2 , which also reflects in S_3 . The phase diagrams show a catastrophic saddle-node bifurcation, where the close-ups at Figure 2 aim to improve the resolution near the critical zone, showing how both stable [blue] and unstable [dashed green] fixed points coincide before transitioning.

Contrasting both figures, the addition of predation ($\alpha \neq 0$) results in the reduction of the area under the bistability surfaces, but not in any change in the dynamics. Stable populations are clearly reduced compared to the cleavage case due to predation's positive effects on S_3 , as the mutant species acts as a limiter for the growth of the system.

For Figure 4 and Figure 5 red phase trajectories lead to extinction, whereas the black ones lead to coexistence. The purple surface delimits the coexistence region of the phase space, as the outcome in the bistable regime depends on the initial conditions. From the shape of the delimiting surface one can see an upper bound for the S_3 population which leads to coexistence. If the S_3 population is too high, the effect of predation/cleavage will be too strong and the system will collapse.

The right-side pictures correspond to a scenario just after the bifurcation has occurred. Although the only stable solution is extinction, phase trajectories passing near the previous fixed point are highly deflected by it, as it is now acting as a *ghost attractor*. This sign of bifurcation memory asymptotically slows down and attracts its near phase trajectories [7][8]. This can be also seen by looking at the respective time trajectories. Excluding

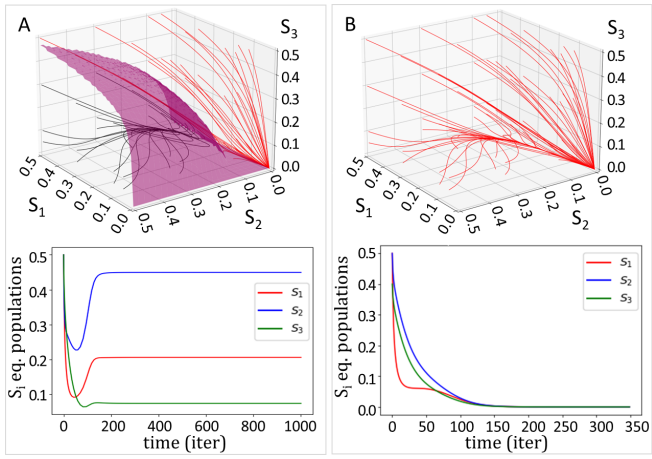


FIG. 4: Phase-space (*top*) and time (*bottom*) trajectories of Eqs. (1) for the case with cleavage, taking $\alpha = 0$. Red phase-space trajectories lead to extinction, black lead to coexistence. The purple surface divides the coexistence and extinction regions of the phase space. *A*: $k_{13} = 0.34$; $k_{21} = 1.0$; $k_{12} = 1.0$; $\mu = 0.4$. This scenario corresponds to bistability. For the time evolution $\vec{S}_0 = (0.5, 0.5, 0.5)$ *B*: $k_{13} = 0.5$; $k_{21} = 1.0$; $k_{12} = 1.0$; $\mu = 0.38$. This scenario corresponds to the extinction zone. For the time evolution $\vec{S}_0 = (0.5, 0.5, 0.4)$

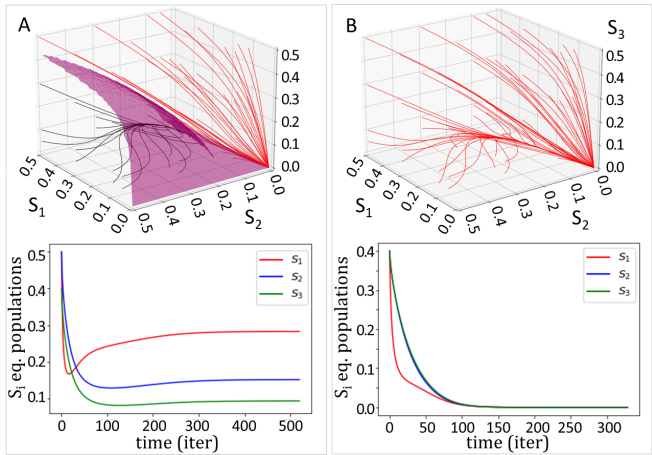


FIG. 5: Phase-space (*top*) and time (*bottom*) trajectories of Eqs. (1) for the predation case, taking $\alpha = 0.75$. *A*: $k_{13} = 0.23$; $k_{21} = 0.5$; $k_{12} = 1.0$; $\mu = 0.25$. This scenario corresponds to bistability. $\vec{S}_0 = (0.5, 0.5, 0.4)$ *B*: $k_{13} = 0.4$; $k_{21} = 0.5$; $k_{12} = 1.0$; $\mu = 0.25$. This scenario corresponds to extinction zone. $\vec{S}_0 = (0.5, 0.5, 0.5)$

the attracting effects of the dominant fixed point, $\vec{S} = \vec{0}$, and the memory effect mentioned above, the trajectories do not show special signs of periodicity nor chaotic behaviour.

The critical behaviour of the system is known to be modeled by the exponential law $t \propto |\phi|^\xi$, where t represents the convergence time, $\phi = \mu - \mu_c$ is the critical parameter for this system. $\xi = -\frac{1}{2}$ for a saddle-node bifurcation [8]. This behaviour has been observed numeri-

cally. For μ values near the critical point, the convergence time iterations behave as expected, for a resolution of 10^7 digits. The numerical value obtained for the critical exponent, $\xi = (-0.499 \pm 0.002)$ agrees with the theoretical value.

B. Spatio-temporal dynamics

Adding spatial correlations can lead to the emergence of interesting phenomena like pattern formation, or to possible changes in the dynamics of the system. Biological systems are inherently tied to a physical 3D or 2D substratum. Thus, to get a better and more realistic understanding of the studied model, a cellular automaton has been programmed for the case with cleavage ($\alpha = 0$). In order to check the correct correspondence between the CA algorithm and the mathematical equations (1), the CA model with suppressed spatial correlations has been compared to the deterministic mean field model dynamics and time evolution (see Figure 6).

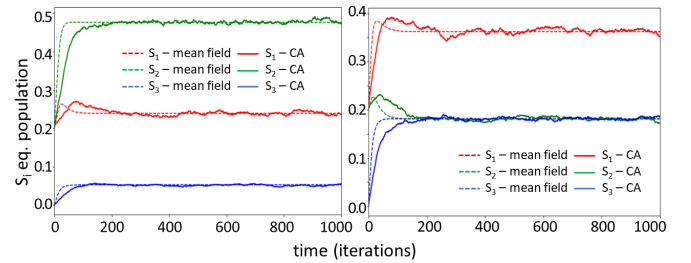


FIG. 6: Comparison between time evolution for the deterministic (dashed lines) and the CA *without spatial correlations* (continuous lines) models. *Right*: $k_{12} = 1.0$; $k_{21} = 1.0$; $k_{13} = 0.0$; $\mu = 0.5$. *Left*: $k_{12} = 0.5$; $k_{21} = 1.0$; $k_{13} = 0.1$; $\mu = 0.1$.

In Figure 7 the results for the CA model with spatial correlations are presented. First, a bifurcation diagram has been computed in terms of the mutation parameter, μ , (main figure) for given initial conditions. As the approach is stochastic, each point represents the mean over several iterations, the error bars being its *statistical deviation*. The dynamics shown in the diagram are similar to the deterministic model, presenting an abrupt saddle-node bifurcation. As expected, the effect of the addition of space and stochasticity has reflected on the critical point values. The upper bound for S_3 population has tightened, leading to a considerably smaller critical point and to smaller S_3 equilibrium population, but not S_2 nor S_1 . Therefore, the spatially correlated model is not a good support for cleaving dynamics.

Also, A and B time evolution sub-plots show that the intensity of the noise due to time and stochasticity rises as the critical point is approached from the left as consequence of the approaching bifurcation. In the two-dimensional space Ω , A and B, one can see the progressive organisation of the species into clusters (better seen

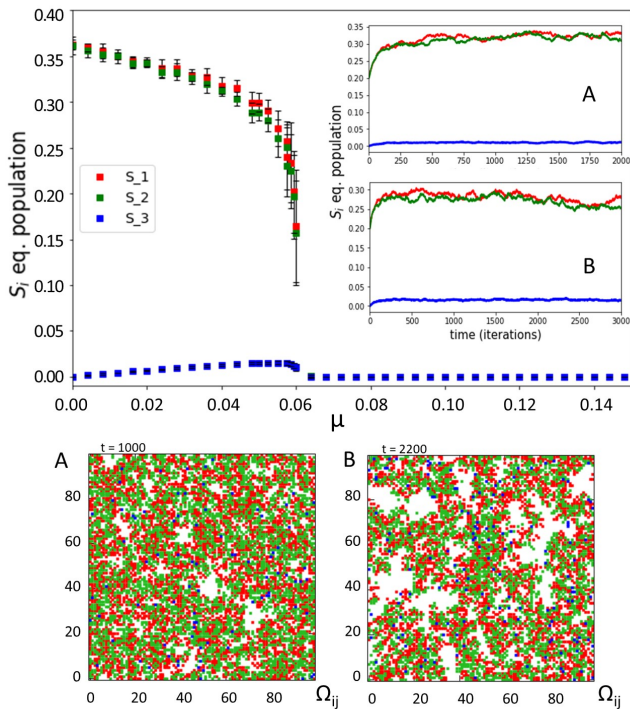


FIG. 7: CA with spatial correlations. The color legend holds for all figures. *Main plot*: Bifurcation diagram for μ with $k_{12} = k_{21} = 1.0$; $k_{13} = 0.1$. The subplots correspond to time evolution (top) and time frame at time t in the $N \times N$, Ω grid, with $N = 100$ (bottom). A: $\mu = 0.03$, $t = 1000$ B: $\mu = 0.055$, $t = 2200$. The bifurcation occurs at $\mu \approx 0.057$.

in B, for smaller equilibrium population near the critical point). It has been seen that the cluster formation is sustained over time iteration in spite of moving due to diffusion.

Therefore, spatial correlations and stochasticity reduce the equilibrium for the cleaving system and introduce cluster pattern formation. This results set a starting point for further research on this approach, needed in order to conclude whether the effects are due to space or

stochasticity by means of Finite Size Scaling, and also to introduce the effects of predation.

IV. CONCLUSIONS

It has been seen from the deterministic analysis that the system presents a catastrophic saddle-node bifurcation for both mutation and cleavage parameters, transitioning from bistability regime to total extinction. The system presents signs of bifurcation memory. In general, the addition of mutation and cleavage effects diminishes the system's stability, as the mutant species acts as a limiter to the coexistence of the system. Nevertheless, there is a short range of values for which stability is, in fact, improved. Thus, the effects of cleavage can be beneficial in small measure due to its growth-control effects over the other species. On the other hand, the addition of predation strongly affects the stability and the equilibrium populations, hence being damaging to the studied system due to the limiting effects of S_3 .

Adding spatial correlations by means of the analysis of the CA model with cleavage has resulted in a strong decrease of the stability of the system, although not to the reduction of S_1 and S_2 population. This shows that the stochastic model has a tighter mutation threshold than the mean field model. Spatially, the species arrange in cluster patterns. Further research is needed in order to fully understand the nature of this effects (stochastic or spatial) and to add the predatory dynamics to the analysis.

Acknowledgments

I would like to thank my supervisors, Dr. Josep Sardanyés and Dr. M. Carmen de Miguel, for all the good advice and guidance throughout this project. Also, my gratitude to my friends and family for all the helpful suggestions and constant support.

-
- [1] M. Eigen, "Selforganization of matter and the evolution of biological macromolecules," *Die Naturwissenschaften*, vol. 58, no. 10, pp. 465–523, 1971.
 - [2] M. Eigen & P. Schuster, "A principle of natural self-organization - Part A: Emergence of the hypercycle," *Naturwissenschaften*, vol. 64, no. 11, pp. 541–565, 1977.
 - [3] N. Vaidya, M. L. Manapat, I. A. Chen, R. Xulvi-Brunet, E. J. Hayden, and N. Lehman, "Spontaneous network formation among cooperative RNA replicators," *Nature*, vol. 491, no. 7422, pp. 72–77, Nov. 2012.
 - [4] H. Klenk et al., "Letters To Nature Through a Hypercyclic Network," *Nature*, vol. 394, no. July, pp. 591–594, 1998.
 - [5] B. Bassols, E. Fontich, D. Oro, D. Alonso, and J. Sardanyés, "Modeling functional shifts in two-species hypercycles."
 - [6] D. Oro, "Breeding biology and population dynamics of Slender-billed Gulls at the Ebro Delta (Northwestern Mediterranean)," *Waterbirds*, vol. 25, no. 1, pp. 67–77, 2002.
 - [7] J. Sardanyés & R. V. Solé, "The role of cooperation and parasites in non-linear replicator delayed extinctions," *Chaos, Solitons and Fractals*, vol. 31, no. 5, pp. 1279–1296, 2007.
 - [8] S. H. Strogatz, *Nonlinear Dynamics and Chaos: With Applications to Physics, Biology, Chemistry and Engineering*. Westview Press, 2000.